IEEE TRANSACTIONS ON

ENERGY CONVERSION

A PUBLICATION OF THE IEEE POWER ENGINEERING SOCIETY

SEPTEMBER 2004 VOLUME 19 NUMBER 3 ITCNE4 (ISSN 0885-8969)

(Contents Continued on Back Cover)

IEEE

(Contents Continued from Front Cover)

DISCUSSIONS AND CLOSURES

CORRECTION

Calculation of Eddy Current Loss in Axial Field Permanent-Magnet Machine With Coreless Stator

Rong-Jie Wang, *Member, IEEE,* and Maarten J. Kamper, *Member, IEEE*

***Abstract*—This paper presents a hybrid method for the calculation of eddy current loss in coreless stator axial field permanent-magnet (AFPM) machines. The method combines the use of two-dimensional finite element (FE) field analysis and the closed-form eddy loss formula. To account for three-dimensional field effects in an AFPM machine, a multilayer and multislice modeling technique has been devised. Experimental tests are carried out to validate the method. It is shown that the proposed method predicts the eddy current losses of a coreless stator AFPM machine with high accuracy.**

***Index Terms*—Axial field, eddy currents, finite-element (FE) method, permanent-magnet (PM) machine.**

I. Introduction

AXIAL FIELD permanent-magnet (AFPM) machines are increasingly being used in amongst others, power generation and light traction drives [1]–[7]. Unlike conventional PM machines, in AFPM machines, the magnetic field is in the axial direction and the stator conductors are radially placed. The typical feature of this topology is that it has a short axial length and large diameter.

One type of AFPM machine is the coreless stator AFPM machine. The stator winding is epoxy encapsulated and located in the air-gap magnetic field generated by magnets mounted on two opposing rotor discs. Fig. 1(a) shows a flat layout on a radial cutting plane over a pole-pitch of such a machine. As is shown, the magnets generate an axial magnetic field component as well as a tangential magnetic field component in the air gap. Motion of the magnets over the winding produces, therefore, alternating fields in the conductors in both the axial and tangential directions, inducing eddy currents as shown in Fig. 1(b). When operating in relatively high-frequency alternating fields, these induced eddy currents may lead to serious additional losses in an AFPM machine increasing the temperature of the windings and decreasing the efficiency of the machine. Predicting the winding eddy losses with high accuracy is, therefore, very important in designing such machines.

According to literature, the standard analytical method derived by Carter [8] has often been used in the design of AFPM machines [1]–[3], [7]. Unfortunately, as pointed out by Sullivan [9], this analytical method has significant limitations as it assumes a one-dimensional (1-D) sinusoidal field and, therefore, will not be accurate enough to represent the true eddy current effects. Although it was mentioned by Caricchi [1] that the loss found by using this formula may be compensated for by multiplying with an empirical factor obtained from a detailed FE study of the flux density in the air gap, there is no further work dealing with this issue in the literature.

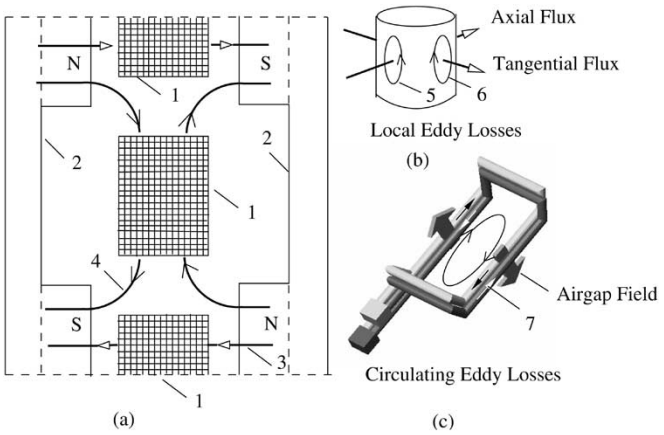

Fig. 1. Eddy current losses in an AFPM machine with a coreless stator topology (a) flat layout of one pole-pitch of the machine, (b) eddy currents in a conductor, (c) circulating current in parallel connected path where 1—phase windings, 2—PM rotor disc, 3—axial field, 4—tangential field, 5—eddy current due to axial flux, 6—eddy current due to tangential flux, 7—circulating current.

In this paper, a hybrid calculation method is presented that can accurately predict the eddy loss in coreless stator AFPM machines. In Section II, the closed-form formula for eddy loss calculation is discussed. In Section III, the hybrid method, termed the finite-element-(FE) aided analytical method, is presented followed by experimental validation in Sections IV and V.

II. Analytical Method

From a machine design perspective, it is desirable to use a simple eddy loss calculation method that can easily be incorporated into the design optimization procedure. The standard method is based on the analytical solution of the eddy loss in a single conductor lying in a transverse alternating field. For a round conductor of diameter d, length l, and resistivity ρ, the eddy current loss P_e is given by [8]

$$P_e = \frac{\pi l d^4 B_{pk}^2 \omega^2}{32\rho} \tag{1}$$

Manuscript received April 15, 2003; revised July 8, 2003. Paper no. TEC-00095-2003. This work was supported in part by the University of Stellenbosch and in part by the SA industry.

The authors are with the Department of Electrical Engineering, University of Stellenbosch, Matieland 7602, South Africa (e-mail: rwang@sun.ac.za; kamper@sun.ac.za).

Digital Object Identifier 10.1109/TEC.2004.832043

where B_{pk} is the peak value of flux density and ω is the electrical angular speed. This is inherently a 1-D analytical method that assumes a sinusoidal field.

As will be shown in Section III, in a coreless stator AFPM machine, the flux density waveform in the air gap is often close to a trapezoidal waveform with an appreciable third and fifth harmonic content [1] and the air-gap magnetic field geometry exhibits a three-dimensional (3-D) nature. Hence, the calculation of the eddy current loss in the stator winding can be subjected to significant error when merely using (1).

It can be seen from (1) that the eddy losses are proportional to d^4. To minimize these eddy current losses, parallel-connected thin conductor wires are often used for the stator coil. However, this may create a new problem [i.e., an eddy circulating current between any two of those parallel paths [10] may occur, as shown in Fig. 1(c)]. To overcome this problem, the normal practice is to twist or transpose the wires in such a fashion that each parallel path occupies all possible layer positions for the same length of the coil. It has been shown in [4] that the circulating currents in an AFPM machine can almost be eliminated by using such a technique.

III. FE-Aided Analytical Method

To take into account 3-D eddy current effects by using a 1-D analytical method, accurate field calculation is essential. Because of the large computing efforts needed in 3-D finite-element (FE) analysis, Two-dimensional (2-D) FE magnetostatic field analysis is performed. It has been assumed in the subsequent analysis that the flux produced by the eddy currents has a negligible influence on the total field and the conductor dimensions are smaller than the skin depth. The eddy current region in the stator winding is thus modeled as a nonconductive area [11].

A. Multilayer FE Model

The 2-D FE modeling of a coreless stator AFPM machine is usually carried out by introducing a radial cutting plane, which is then developed into a 2-D flat model. Fig. 2 shows an FE mesh for such a model, which spans one pole-pitch of the AFPM machine. The air-gap region was modeled using the Cartesian air-gap element (CAGE) as described in [12]. Having solved the FE model, it is possible to extract both normal and tangential field values along contours C1, C2, and C3 as plotted in Figs. 3 and 4, respectively.

It can readily be observed that for a coreless stator AFPM machine, the amplitudes of both the normal and tangential field components vary greatly with air-gap position and the flux density waveforms contain a significant amount of harmonics. Since $P_e \propto B_{pk}^2$ (1), eddy current loss in the individual conductors depends, therefore, upon their positions in the air gap. The conductor nearer the face of the magnet experiences higher flux densities and, therefore, has large induced eddy current loss.

Assuming that one can mesh the phase winding area into a number of thin *layers*, which are bar-shaped areas as illustrated in Fig. 5(a), the nodes on the top and bottom boundaries will be equally spaced and distributed resulting in many small subdivided rectangular regions on each layer. Given the nodal vector potential values from a field solution, the axial and tangential flux densities (B_x, B_y) of a small subregion n as shown in Fig. 5(b) may be determined by using

$$\begin{cases} B_x = \frac{1}{2}\left[\frac{A_1 - A_3}{dy} + \frac{A_2 - A_4}{dy}\right] \\ B_y = \frac{1}{2}\left[\frac{A_1 - A_2}{dx} + \frac{A_3 - A_4}{dx}\right]. \end{cases} \tag{2}$$

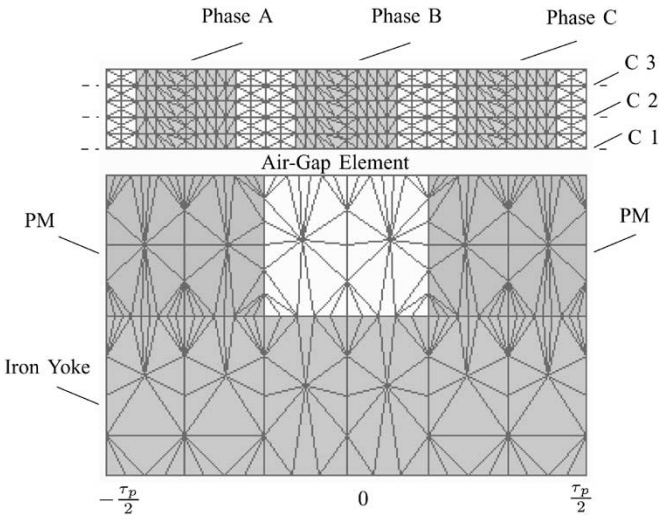

Fig. 2. The 2-D FE model of a coreless stator AFPM machine.

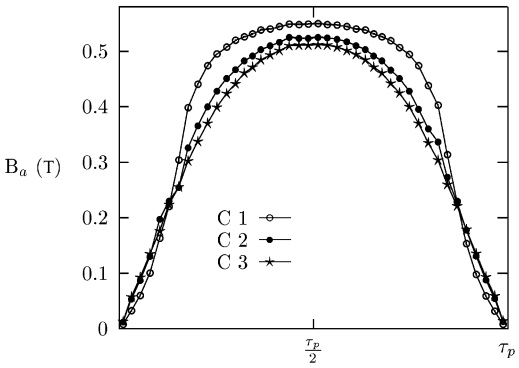

Fig. 3. Comparison of air-gap axial flux density distribution at different conductor positions across the air gap (C1, C2, C3 of Fig. 2).

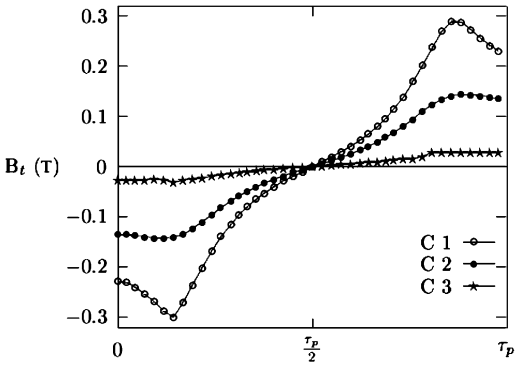

Fig. 4. Comparison of air-gap tangential flux density distribution at different conductor positions across the air gap (C1, C2, C3 of Fig. 2).

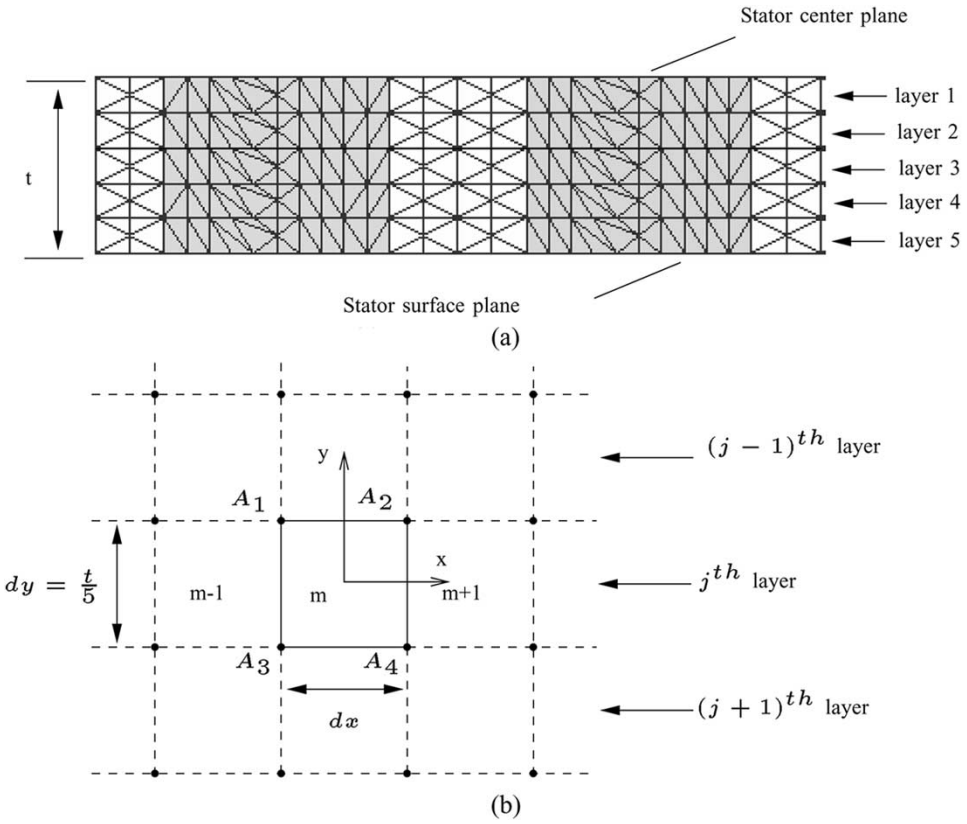

Fig. 5. The two-dimensional multilayer FE model.

where A_1–A_4 are nodal vector potential values. With the flux densities of each subregion calculated, the flux density waveform of a conductor layer is obtained, which is Fourier analyzed to determine the amplitude of each flux density harmonic component. In this way, the eddy losses due to the high-order harmonic components of the flux density are accounted for. The total eddy current loss P_s in a conductor can thus be computed by using (1), that is

$$P_s = \frac{\pi l_r d^4 \omega_1^2}{32\rho} \sum_{i=1}^{n} i^2 \left(Bx_i^2 + By_i^2\right) \tag{3}$$

where l_r is the radial length of the conductor, Bx_i and By_i are the tangential and axial peak flux densities of the ith-order harmonic, respectively, and ω_1 is the fundamental angular frequency.

Since individual conductors in a conductor layer experience the same flux density waveform and, thus, have the same eddy loss, the eddy loss of each conductor layer may be obtained by adding the eddy loss in each conductor. Assuming that there are n_j conductors in a conductor layer j, the overall eddy loss P_j of conductor layer j may be given by

$$P_j = n_j \cdot P_s = \frac{\pi l_r d^4 \omega_1^2}{32\rho} \cdot n_j \sum_{i=1}^{n} i^2 \left(Bx_i^2 + By_i^2\right). \tag{4}$$

It follows that if there are l conductor layers in the eddy current region, the overall eddy loss P_{le} of all conductors is given by

$$P_{le} = \sum_{j=1}^{l} P_j = \frac{\pi l_r d^4 \omega_1^2}{32\rho} \sum_{j=1}^{l} n_j \sum_{i=1}^{n} i^2 \left(Bx_{ij}^2 + By_{ij}^2\right) \tag{5}$$

where Bx_{ij} and By_{ij} are ith-order components of the tangential and axial peak flux densities of the jth conductor layer, respectively.

The effects of both fundamental and harmonic air-gap flux components to the eddy current loss are compared in Table I, in which eddy losses due to fundamental flux P_{je1} and due to harmonic flux components $\sum_{i=2}^{n} P_{jei}$ in conductor layer j [Fig. 5(a)] are normalized to the total eddy loss P_{le}. It is clear that these losses vary significantly from one layer to another. Approximately 18% of total eddy loss is attributed to the harmonic components of the flux waveform. It is thus important to take into account these harmonic eddy losses in the eddy loss calculation.

B. Computational Limitations of 2-D FE Modeling

Unlike a conventional electrical machine, the field geometry in an AFPM machine varies at different radii. Imagine that one can cut a section (equivalent to one pole-pitch of the machine) out of an AFPM machine as shown in Fig. 6, and then further divide it into several sectors. Each sector may be unfolded and represented by a 2-D flat FE model (hereafter referred to as *slices*).

TABLE I
NORMALIZED EDDY LOSSES IN DIFFERENT CONDUCTOR LAYERS

Number of layer	P_{je1}/P_{le}	$\sum_{i=2}^{n} P_{jei}/P_{le}$
1^{st}	13.7%	1.8%
2^{nd}	14.4%	2.1%
3^{rd}	15.7%	2.7%
4^{th}	17.7%	4.1%
5^{th}	20.4%	7.4%
Total	81.9%	18.1%

It can be seen from Fig. 6 that these 2-D FE models are noticeably different. As for an example, the inner slice 3 has a much smaller interpole gap than that of the outer slice 1.

After solving these 2-D FE models, the air-gap flux distribution of each slice is obtained and plotted on the same coordinate system as shown in Figs. 7 and 8. Despite the fact that the variation of flux density waveform of each slice is not as great as that of each layer for this particular machine, it is clear that FE modeling of a coreless stator AFPM machine is inherently a 3-D problem and a simple 2-D FE model may not be an accurate representation of the problem. This is particularly important when it comes to the eddy current loss calculation as a small variation in the flux density may lead to a significant error. The uneven distribution of eddy losses in different slices has been investigated in [4] and it showed that harmonic eddy loss in the slice of smaller radius may be significantly higher (20%) than that in the slice of a larger radius.

C. Including 3-D Effects in 2-D FE Analysis

The use of a 2-D FE model indicates that 3-D features of the field distribution can only be represented in an approximate manner. The proposed approach accounts for 3-D field effects of an AFPM machine by using a sequence of 2-D FE submodels (*slices*) as shown in Fig. 6.

The alignments of the rotors and stators of each successive slice are indexed to reflect the variation in the field distribution at different radii. If there are s such slices, and all are assumed to have the same radial length l_r, then the effective value of the eddy loss in the stator P_{se} is

$$P_{se} = \frac{1}{s}\sum_{k=1}^{s} P_{(le)k} \tag{6}$$

where $P_{(le)k}$ is the eddy current loss of the kth slice calculated by (5). On substitution of (5), the above equation is then

$$P_{se} = \frac{\pi l_r d^4 \omega_1^2}{32\rho s}\sum_{k=1}^{s}\sum_{j=1}^{l} n_j \sum_{i=1}^{n} i^2\left(Bx_{ijk}^2 + By_{ijk}^2\right). \tag{7}$$

Obviously, using this method will require several field solutions to be performed at the same rotor position (e.g., the three-slice FE model needs three 2-D FE solutions), which will be computationally expensive if a complicated FE model has to be solved. However, considering the relatively simple geometry of coreless stator AFPM machines (Fig. 2), the computation efforts involved in solving such a 2-D FE model are usually modest, even more so when a judicious selection of the boundary conditions and the modeled area are possible. The typical CPU time for solving such a FE model on a Celeron 333-MHz computer running Redhat Linux operating system is about 5 s.

Combining the 2-D multilayer FE model with the multislice FE model, the 3-D effects of the eddy loss in an AFPM machine

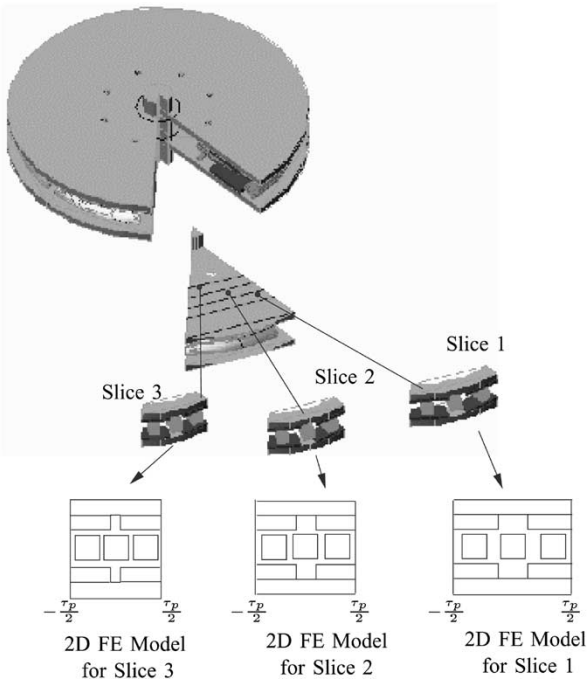

Fig. 6. Two-dimensional multislice FE model of an AFPM machine.

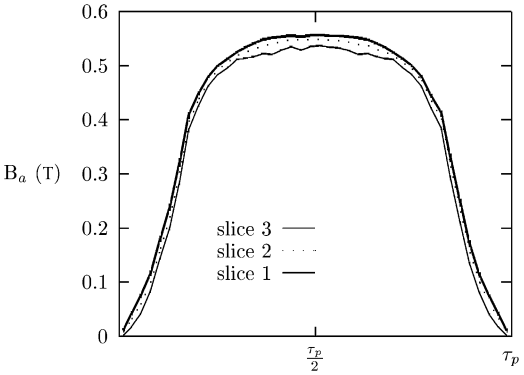

Fig. 7. Comparison of air-gap axial flux distribution of different slices.

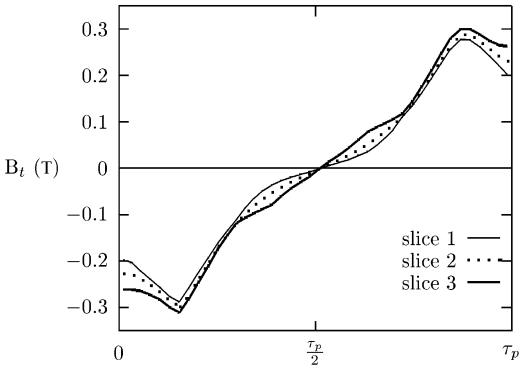

Fig. 8. Comparison of air-gap tangential flux density distribution of different slices.

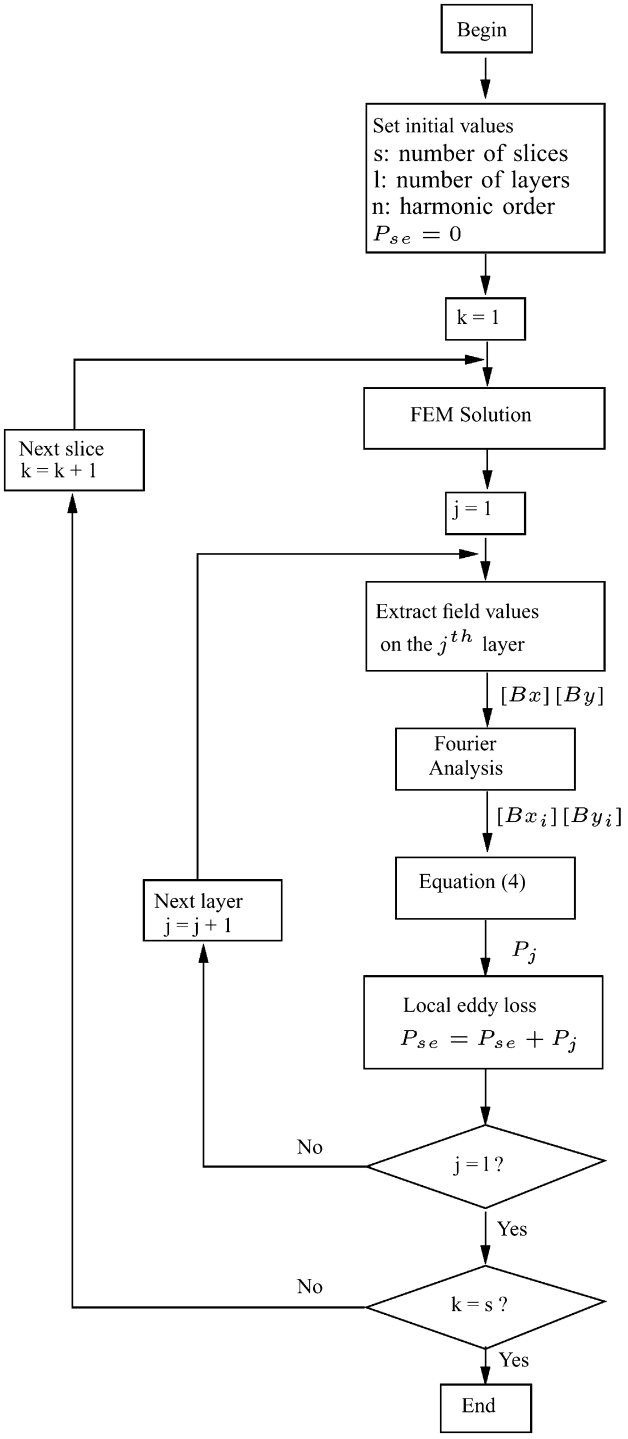

Fig. 9. FE calculation of eddy loss taking into account 3-D effects.

may be represented in a 2-D fashion. Fig. 9 shows the procedures of the implementation of the proposed modeling.

IV. Experimental Validation

The resistance-limited eddy loss in the stator of an AFPM machine may be experimentally determined by measuring the difference in input shaft powers of the AFPM machine at the same speed, first with the stator in, and then replacing it with a dummy stator (without conductors). The dummy stator has the same dimensions and surface finish as the real stator and is used to ensure that the windage losses are the same in both cases.

A schematic representation of the experimental test setup for measuring eddy losses is shown in Fig. 10. The experimental prototype and driving machine are connected via a torque sensor. To eliminate the effects of possible eddy-circulating current in the windings and eddy current loss in the end-windings caused by end-winding flux linkages, the coils are replaced by bunches of conductors, which are of the same length as the PMs.

All of the conductor groups are symmetrically placed in a mould and then epoxy encapsulated to form a coreless stator. A few temperature sensors are also attached to the conductors in order to measure the conductor temperature to be used in the theoretical calculation. Fig. 11 shows the measured and calculated resistance limited eddy loss of the prototype machine. It is seen that the eddy loss calculated by using the standard analytical method (1) alone gives very much underestimated values (43% less in this case). A high accuracy, however, is achieved by using the developed technique. In the calculation, five layers have been used for each slice to account for 2-D field effects.

Note that the improvement of accuracy from a three-slice (3 FE solutions) to a five-slice (5 FE solutions) model is not as significant as compared to from a one-slice to a three-slice model. It may be a good tradeoff between accuracy and CPU time to use a three-slice FE model.

TABLE II
Design Data for the AFPM Machine Under Study

Rated line voltage	550 V (Star connection)
Rated phase current	320 A
Number of poles	40
Rated speed	2300 rpm
Axial length	72 mm
Outer diameter	720 mm
Inner diameter	500 mm
Magnet shape	Trapezoidal
Pole arc/pole pitch	0.72
Air-gap clearance	2.75 mm
Number of coils	60
Type of winding	Single layer trapezoidal
Turns per coil	51
Connection	20 parallel circuits/phase
Conductor	12 parallel wires/coil (twisted)

V. Application

The above-described modeling technique has been applied to the design and optimization of a 300-kW AFPM generator. Fig. 12 shows the prototype AFPM generator manufactured at the electrical machines laboratory of the University of Stellenbosch, South Africa. The design data of the AFPM generator are given in Table II.

The resistance limited eddy loss of this machine is measured according to the same procedure as described in Section IV.

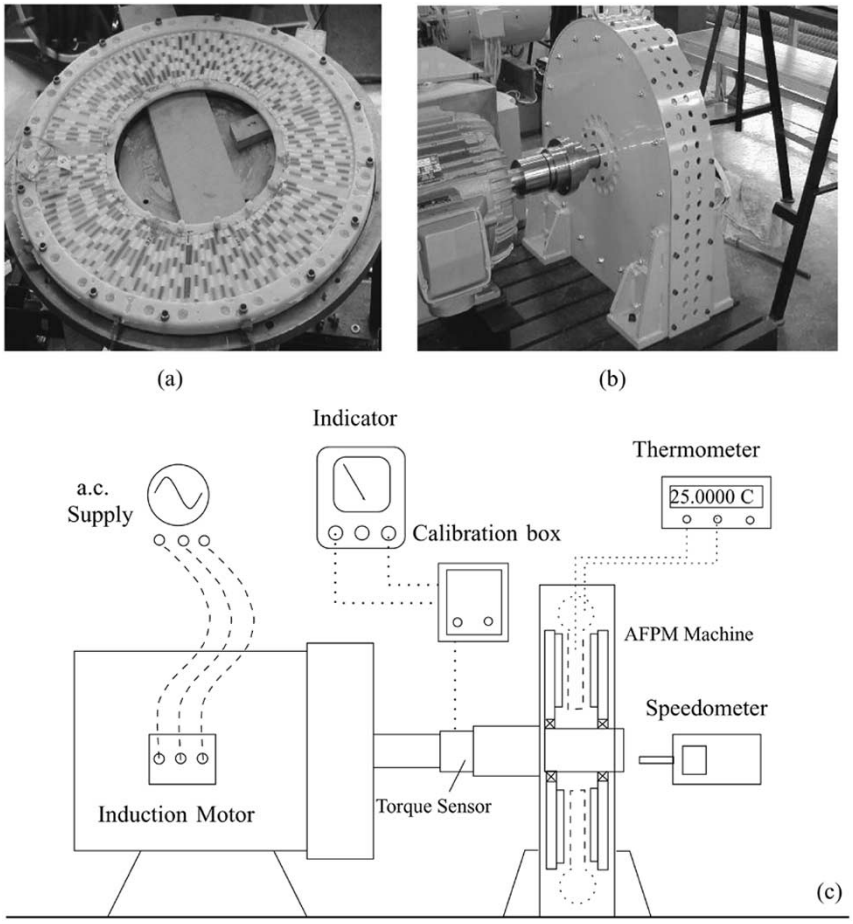

Fig. 10. Laboratory setup for measuring the eddy current loss, where (a) is a specially designed dummy stator, (b) is the experimental machine, and (c) is a schematic representation of the experimental setup.

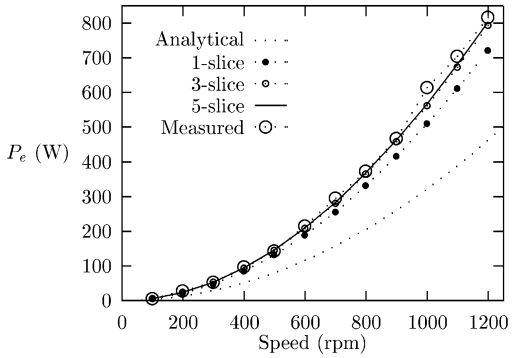

Fig. 11. Comparison of calculated eddy loss with measurements.

As shown in Table II, the stator winding of the prototype AFPM machine consists of 20 parallel coils per phase. To avoid the inclusion of possible eddy circulating current loss in the measurement, the parallel coils of each phase were disconnected. Fig. 13 compares the measured and predicted eddy current losses using the developed technique. The calculated eddy loss agrees very well with the measurements. This confirms that the standard eddy loss formulation enhanced by the multislice and multilayer FE field model can predict eddy current loss in an AFPM machine accurately.

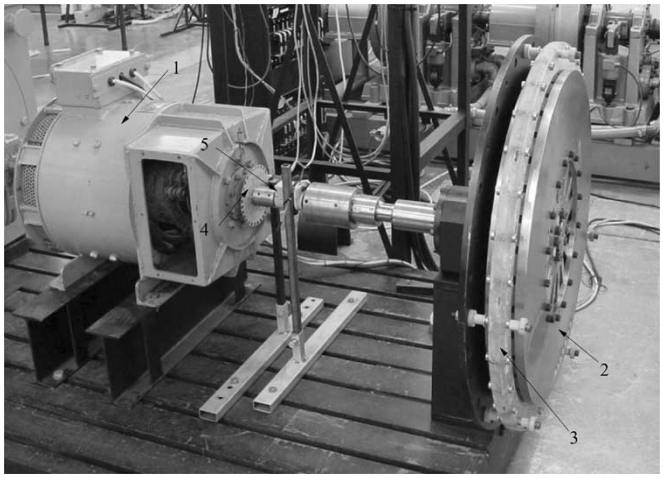

Fig. 12. Experimental setup for eddy loss measurements of a 300-kW AFPM machine, where 1—dc machine, 2—rotor disc of the AFPM machine, 3—stator, 4—speed measurement disk, and 5—torque sensor.

VI. Conclusion

A combined model utilizing an analytical method and a 2-D FE solution has been fully developed for the accurate calculation of eddy current loss in coreless stator AFPM machines. The proposed method allows for the calculation of eddy losses

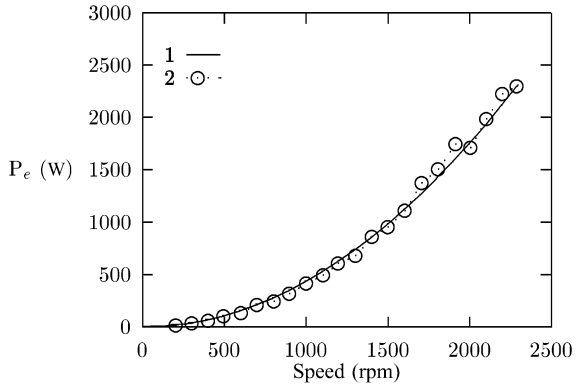

Fig. 13. Measured and calculated eddy current loss versus rotating speed, where 1—calculated eddy loss by using the multislice and multilayer FE model, and 2—measured eddy loss.

in generic AFPM machines taking into account 2-D and 3-D effects and nonsinusoidal field distribution in both the axial and tangential directions.

The new hybrid method has been validated thoroughly with good correlation between measured and calculated results. It was found that 3–5 slices are normally enough to use in the calculation. It is further shown that the analytical method alone gives very much underestimated values.

REFERENCES

[1] F. Caricchi, F. Crescimbini, O. Honorati, G. L. Bianco, and E. Santini, "Performance of core-less winding axial-flux PM generator with power output at 400 Hz—3000 rev/min," *IEEE Trans. Ind. Applicat.*, vol. 34, pp. 1263–1269, Nov./Dec. 1998.

[2] L. Soderlund, A. Koski, H. Vihriala, J. T. Eriksson, and R. Perala, "Design of an axial flux permanent magnet wind power generator," in *Proc. 8th Int. Conf. Electrical Machine and Drives*, 1997, pp. 224–228.

[3] E. Spooner and B. J. Chalmers, "TORUS: A slotless, toroidal-stator, permanent-magnet generator," *Proc. Inst. Elect. Eng. B*, vol. 139, no. 6, pp. 497–506, 1992.

[4] R. Wang, "Design Aspects and Optimization of an Axial Field Permanent Magnet Machine With an Ironless Stator," Ph.D. dissertation, Dept. Elect. Eng., Univ. Stellenbosch, Matieland, South Africa, 2003.

[5] N. F. Lombard and M. J. Kamper, "Analysis and performance of an ironless stator axial flux PM machine," *IEEE Trans. Energy Conversion*, vol. 14, pp. 1051–1056, Dec. 1999.

[6] F. Caricchi, F. Crescimbini, E. Fedeli, and G. Noia, "Design and construction of a wheel-directly-coupled axial-flux PM motor prototype for EVs," in *Proc. IEEE Ind. Applicat. Soc. Annu. Meeting*, 1994, pp. 254–261.

[7] H. C. Lovatt, V. S. Ramdenand, and B. C. Mecrow, "Design an in-wheel motor for a solar-powered electric vehicle," *Proc. Inst. Elect. Eng., Electric Power Applicat.*, vol. 145, no. 5, pp. 402–408, 1998.

[8] G. W. Carter, *Electromagnetic Field in its Engineering Aspects*. White Plains, NY: Longman, 1954.

[9] C. R. Sullivan, "Computationally efficient winding loss calculation with multiple windings, arbitrary waveforms, and two-dimensional or three-dimensional field geometry," *IEEE Trans. Power Electron.*, vol. 16, pp. 142–150, Jan. 2001.

[10] M. G. Say, *Alternating Current Machines*. New York: Pitman, 1983.

[11] S. J. Salon, *Finite Element Analysis of Electrical Machines*. MA: Kluwer, 1995.

[12] R. Wang, H. Mohellebi, T. J. Flack, M. J. Kamper, J. Buys, and M. Feliachi, "Two-dimensional Cartesian air-gap element (CAGE) for dynamic finite-element modeling of electrical machines with a flat air gap," *IEEE Trans. Magn.*, vol. 38, pp. 1357–1360, Mar. 2002.

Rong-Jie Wang (M'00) received the M.Sc. (Eng.) degree from the University of Cape Town, Cape Town, South Africa, in 1998 and the Ph.D. (Eng.) degree from the University of Stellenbosch, Matieland, South Africa, in 2003.

Currently, he is a Postdoctoral Research Fellow in the Department of Electrical Engineering, University of Stellenbosch. His research area is on special electrical machines, design optimization of electrical machines using FE method, thermal modeling of electrical machines, and renewable energy systems. He has published several journal and conference papers on the design and analysis of special electrical machines such as axial field PM machines and linear machines.

Maarten J. Kamper (M'96) received the M.Sc. and Ph.D. degrees in engineering from the University of Stellenbosch, Matieland, South Africa, in 1987 and 1996, respectively.

Currently, he is a Professor in the Department of Electrical Engineering at the University of Stellenbosch, where he has been since 1989. He was a Researcher with the SA Transport Services and the SA Council for Scientific and Industrial Research (CSIR), Pretoria, South Africa, for several years. His research area is on computer-aided design and control of reluctance synchronous, switched reluctance, and PM machine drives. He is a South African National Research Foundation (NRF)-supported scientist and has published many journal and conference papers on various topics of electrical machines.